(2)

ARMY RESEARCH LABORATORY

Helicopter Forced Response Vibration Analysis Method RTVIB20

Joseph Fries

ARL-TR-75 February 1993

APPROVED FOR PUBLIC RELEASE; DISTRIBUTION IS UNLIMITED.

NOTICES

REPORT DOCUMENTATION PAGE

Form Approved
OMB No. 0704-0188

1. AGENCY USE ONLY *(Leave blank)*

2. REPORT DATE
February 1993

3. REPORT TYPE AND DATES COVERED
Final, Jan 90–Jun 92

4. TITLE AND SUBTITLE
Helicopter Forced Response Vibration Analysis Method RTVIB20

5. FUNDING NUMBERS
WO: 44592-202-94-2123
PR: 1L162618AH80

6. AUTHOR(S)
Joseph Fries

7. PERFORMING ORGANIZATION NAME(S) AND ADDRESS(ES)

8. PERFORMING ORGANIZATION REPORT NUMBER

9. SPONSORING/MONITORING AGENCY NAME(S) AND ADDRESS(ES)
U.S. Army Research Laboratory
ATTN: AMSRL-OP-CI-B (Tech Lib)
Aberdeen Proving Ground, MD 21005-5066

10. SPONSORING/MONITORING AGENCY REPORT NUMBER
ARL-TR-75

11. SUPPLEMENTARY NOTES

12a. DISTRIBUTION/AVAILABILITY STATEMENT
Approved for public release; distribution is unlimited

12b. DISTRIBUTION CODE

13. ABSTRACT *(Maximum 200 words)*

This report describes a helicopter vibration analysis method. In this method, the rotor forcing for a single main rotor is calculated by integrating the forces and moments at the rotor center, and then applying them to a rigid helicopter airframe. The vibrations (any place in the airframe) are calculated as the response to the applied hub center forces and moments. The method of analysis allows for dissimilar blades in the main rotor to simulate various types of blade damage and the resulting increase in vibrations transmitted into the airframe. The analysis method is generic and can be used to analyze any single main rotor helicopter. An application is made for the UH-60A helicopter, resulting from the loss of outboard sections of one blade of the rotor, and the resulting vibrations in the cockpit are calculated.

14. SUBJECT TERMS
rotor blades; aerodynamic forces; vibrations; helicopters; vibration analysis

15. NUMBER OF PAGES
31

16. PRICE CODE

17. SECURITY CLASSIFICATION OF REPORT	18. SECURITY CLASSIFICATION OF THIS PAGE	19. SECURITY CLASSIFICATION OF ABSTRACT	20. LIMITATION OF ABSTRACT
UNCLASSIFIED	UNCLASSIFIED	UNCLASSIFIED	SAR

INTENTIONALLY LEFT BLANK.

TABLE OF CONTENTS

INTENTIONALLY LEFT BLANK.

1. INTRODUCTION

This report describes an analytical method and its associated computer program which can be used to predict helicopter vibrations for undamaged and damaged main rotor blades. The analysis is generic and can be used to analyze any helicopter with a minimal amount of physical input data.

The model consists of independent main rotor blade flapping-torsional degrees of freedom and helicopter longitudinal-vertical degrees of freedom. Level flight trimmed conditions are determined first, after which damage is imposed onto the main rotor blades. Vibration levels are calculated in the cockpit both for the undamaged and damaged cases. The model considers aerodynamic forces and moments using blade element theory wherein each harmonic is calculated individually.

This program calculates cockpit vibrations for a bare helicopter with no vibration absorber devices present, and, in conjunction with input of human tolerance to vibration data, the code can be used to predict aircraft kill categories.

There are other sources contributing to helicopter vulnerability due to main rotor blade damage besides human vibration tolerance, which can also place a helicopter in jeopardy. These include loss of main rotor blade structural integrity, vibrations transmitted to other critical structural components on the aircraft, and lack of pilot control authority to compensate for blade damage. These additional factors are not included in this analysis.

The aerodynamic terms are developed using blade element theory in Section 3 and are referenced to Figure 1. The basic theory is from Barnes (1967) and Chopra (1992). In this analysis, the aerodynamic forcing functions are separated into individual harmonics so as to be able to trace the frequency filtering effect from the rotating blade into the fixed (fuselage) system and to isolate and identify the fundamental physical parameter contributions to the aerodynamic forcing functions.

Section 4 describes results of application of the analysis to a UH-60A helicopter in which one blade in the main rotor is considered to be damaged. The damage consists of the removal of various amounts of the outboard end (tip) portions of one rotor blade. Section 5 discusses the results of the damaged rotor blade analyses, and Section 6 draws conclusions from the results.

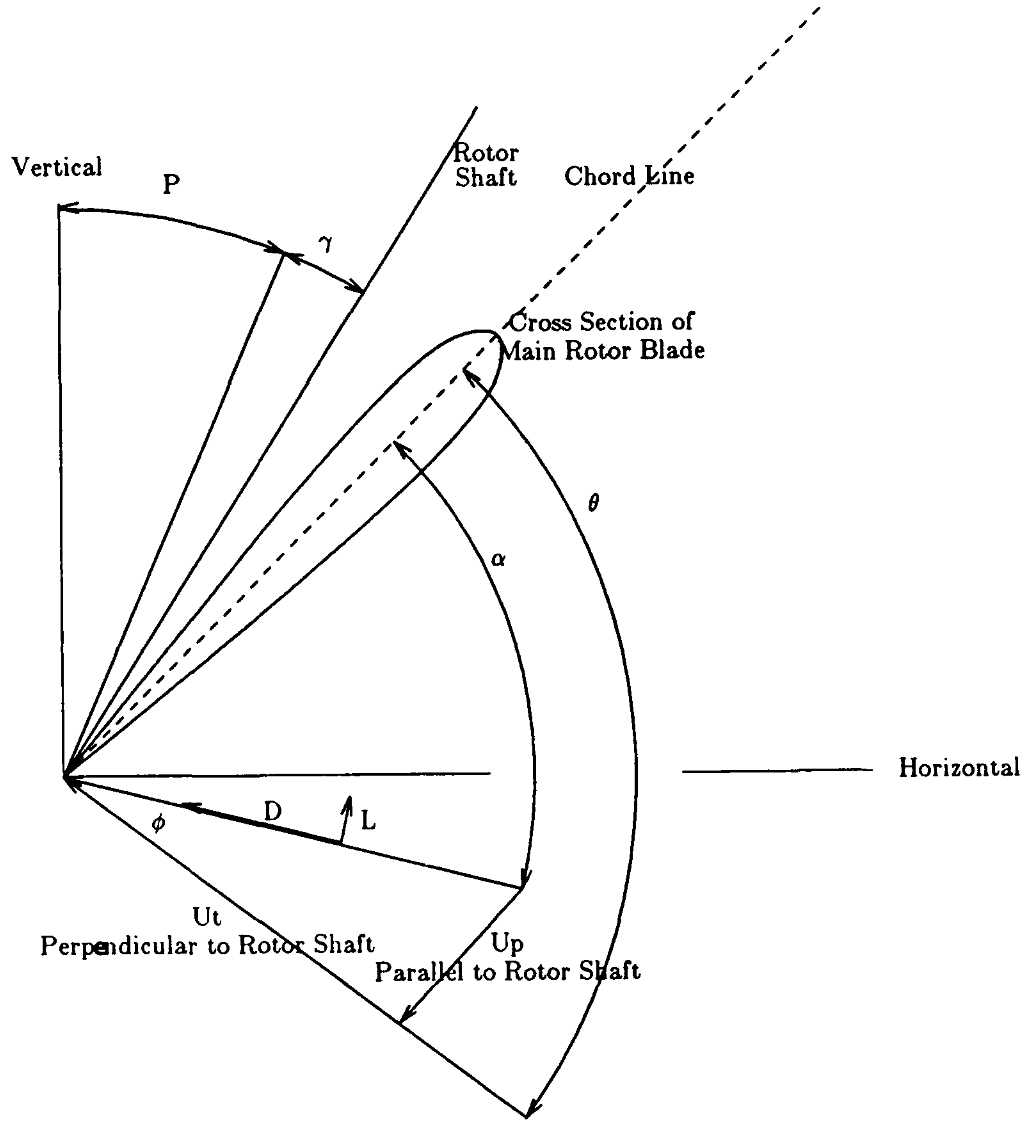

Figure 1. Aerodynamic airfoil definitions.

The Appendix contains a description of the code, the input variables required, a description of the computer code output, and a list of output variables.

2. NOMENCLATURE

α	Angle of attack
a	Lift slope
β	Flap angle
c	Chord
C_d	Blade drag coefficient
C_l	Blade lift coefficient
C_m	Blade torsional moment coefficient
L	Lift
D	Drag
e_a	Blade torsional elastic axis, + measured from PA toward leading edge
F	Force parallel to rotor shaft
F_o	Steady value of F
γ	Rotor shaft built in tilt angle + forward
Ω	Rotor speed
P	Helicopter pitch angle + into the wind
PA	Blade pitch axis, + measured from leading edge
Π	Pi = 3.14
Ψ	Rotor azimuth angle
r	Variable blade radius
R	Blade radius
ρ	Air density
t	Time
θ	Pitch angle
U	Average downwash velocity
X	Helicopter longitudinal displacement
Z	Helicopter vertical displacement
N	Number of blades per rotor
Q	Coefficient of α^2 in C_m equation
K	Harmonic Number

3. DERIVATION OF AERODYNAMIC TERMS

The rotor blade lift and drag per unit length is defined as*

$$\frac{dL}{dr} = \frac{1}{2}\,\rho\, C_l\, c\,(U_T^2 + U_P^2) \tag{1}$$

and

$$\frac{dD}{dr} = \frac{1}{2}\,\rho\, C_D\, c\,(U_T^2 + U_P^2)\,, \tag{2}$$

where

$$C_l \;=\; \alpha a, \quad \alpha = \theta - \phi\,, \tag{3}$$

$$\phi \;=\; TAN^{-1}\left(\frac{U_P}{U_T}\right), \tag{4}$$

$$U_T \;=\; \Omega r + \left(\frac{dX}{dt}\, COS\,(P+\gamma) \;-\; \frac{dZ}{dt}\, SIN\,(P+\gamma)\, SIN\,\Psi\right), \tag{5}$$

$$U_P \;=\; U + \frac{dX}{dt}\, SIN\,(P+\gamma) \;+\; \frac{dZ}{dt}\, COS\,(P+\gamma) \;+\; \frac{r d\beta}{dt}\,, \tag{6}$$

$$\theta \;=\; \sum_{i=o}^{K} \theta_{ic}\; COS\, i\Psi \;+\; \theta_{is}\; SIN\, i\Psi\,, \tag{7}$$

and

$$\beta \;=\; \sum_{i=o}^{K} \beta_{ic}\; COS\, i\Psi \;+\; \beta_{is}\; SIN\, i\Psi\,. \tag{8}$$

Resolving *dL/dr* and *dD/dr* parallel to the rotor shaft,

$$\frac{dF}{dr} = \frac{dL}{dr}\, COS\,\phi - \frac{dD}{dr}\, SIN\,\phi\,. \tag{9}$$

* Equations 1 to 4 are standard blade element theory equations from Barnes (1967) and Chopra (1992). The equations 5 to 42 were developed by the author.

For high-speed level flight, $\phi = U_P/U_T$, then

$$\frac{dL}{dr} = \frac{1}{2}\rho\, ac\left(U_T^2 + U_P^2\right)\left(\theta - \frac{U_P}{U_T}\right). \tag{10}$$

Also for level flight, let $COS\phi = 1$ and $SIN\phi = \phi$, so that

$$\frac{dF}{dr} = \frac{1}{2}\rho\, ac\left[\theta\left(U_T^2 + U_P^2\right) - U_P\, U_T\right] - \frac{1}{2}\rho\, C_D\, c\, U_P U_T, \tag{11}$$

where terms of third order are neglected

$$\frac{U_P^3}{U_T}.$$

Collecting terms

$$\frac{dF}{dr} = \frac{1}{2}\rho c\left[a\theta\left(U_T^2 + U_P^2\right) - U_T\, U_P\, (a + C_D)\right]. \tag{12}$$

U_T and U_P are written as

$$U_T = \Omega r + \left(\frac{dX}{dt} - \frac{dZ}{dt}(P+\gamma)\right) SIN\ \Psi \tag{13}$$

and

$$U_P = U + \frac{dX}{dt}(P+\gamma) + \frac{dZ}{dt} + \frac{rd\beta}{dt}. \tag{14}$$

The downwash velocity is calculated as

$$U = \sqrt{\frac{NF_o}{2\rho\Pi R^2}}. \tag{15}$$

For level high-speed flight, $U_P << U_T$, so Equation 12 can be written as

$$\frac{dF}{dr} = \frac{1}{2}\rho c \left[a\theta U_T^2 - U_T U_P (a + C_D)\right] . \qquad (16)$$

Define the following parameters:

$$AU = \frac{dX}{dt} - \frac{dZ}{dt}(P + \gamma) , \qquad (17)$$

$$BU = \Omega^2 r^2 + \frac{(AU)^2}{2} , \qquad (18)$$

$$DU = 2\Omega r(AU) , \qquad (19)$$

$$EU = \frac{-(AU)^2}{2} , \qquad (20)$$

and

$$GU = U + \frac{dX}{dt}(P + \gamma) + \frac{dZ}{dt} . \qquad (21)$$

This allows

$$U_T^2 = (BU) + (DU)SIN\Psi + (EU)COS2\Psi \qquad (22)$$

and

$$U_T U_P = \Omega r(GU) + \Omega r^2 \frac{d\beta}{dt} + (AU)(GU)SIN\Psi + (AU)r\frac{d\beta}{dt}SIN\Psi . \qquad (23)$$

Performing a radial integration of the terms containing r, evaluating the trigonometric product terms, and substituting in Equation 16, we obtain new harmonic terms that are sums and differences of the original harmonic products. This is called harmonic cross coupling.

$$F = \frac{1}{2}\rho c \left(a\Omega^2 \frac{R^3}{3} + (AU)^2 \frac{R}{2} \right) \sum_{i=o}^{K} \theta_{ic} \, COS \, i\Psi$$

$$+ a\left(\Omega^2 \frac{R^3}{3} + (AU)^2 \frac{R}{2}\right) \sum_{i=o}^{K} \theta_{is} \, SIN \, i\Psi$$

$$+ a\Omega R^2 \frac{(AU)}{2} \sum_{i=o}^{K} \theta_{ic} \left[SIN(i+1)\Psi - SIN(i-1)\Psi\right]$$

$$+ a\Omega R^2 \frac{(AU)}{2} \sum_{i=o}^{K} \theta_{is} \left[COS(i-1)\Psi - COS(i+1)\Psi\right]$$

$$- a\,(AU)^2 \frac{R}{4} \sum_{i=o}^{K} \theta_{ic} \left[COS(i+2)\,\Psi + COS(i-2)\Psi\right]$$

$$- a\,(AU)^2 \frac{R}{4} \sum_{i=o}^{K} \theta_{is} \left[SIN(i+2)\Psi + SIN(i-2)\Psi\right]$$

$$- (a + C_D) \frac{\Omega}{2} R^2 (GU)$$

$$- (a + C_D) R^3 \frac{\Omega^2}{3} \sum_{i=o}^{K} i\left(-\beta_{ic} SIN\, i\Psi + \beta_{is} COS\, i\Psi\right)$$

$$- (a + C_D)(AU)(GU) R \; SIN\Psi$$

$$- (a + C_D)(AU) \frac{R^2}{2} \Omega \sum_{i=o}^{K} \frac{-i\beta_{is}}{2} \left[COS(i-1)\Psi - COS(i+1)\Psi\right]$$

$$- (a + C_D)(AU) \frac{R^2}{2} \Omega \sum_{i=o}^{K} \frac{i\beta_{is}}{2} \left[SIN(i+1)\Psi - SIN(i-1)\Psi\right]. \qquad (24)$$

For torsion, the moment per unit span is

$$\frac{dM}{dr} = \frac{1}{2} \rho\, C_M c^2 \left(U_T^2 + U_P^2\right), \qquad (25)$$

where

$$C_M = C_{M0} + \gamma\alpha + Q\alpha^2 \, , \tag{26}$$

$$C_M = C_{M0} + \gamma\left(\theta - \frac{U_P}{U_T}\right) + Q\left(\theta - \frac{U_P}{U_T}\right)^2 , \tag{27}$$

and

$$\frac{dM}{dr} = \frac{1}{2}\rho c^2 \left(C_{M0}\, U_T^2 + \gamma\theta U_T^2 - \gamma U_T U_P + Q\theta^2 U_T^2 - 2Q\theta U_T U_P\right) . \tag{28}$$

After integrating radially along the blade and separating out harmonics similar to the harmonic cross coupling that was obtained for the force terms F of Equation 24.

$$M = \frac{1}{2}\rho c^2 C_{M0}\left[\left(\Omega^2\frac{R^3}{3} + (AU)^2\frac{R}{2}\right) + \Omega R^2 (AU) SIN\Psi - (AU)^2\frac{R}{2} COS 2\Psi\right]$$

$$+\frac{1}{2}\rho c^2\gamma\left[\left(\Omega^2\frac{R^3}{3} + (AU)^2\frac{R}{2}\right)\sum_{i=o}^{K}\theta_{ic} COS\, i\Psi\right]$$

$$+\frac{1}{2}\rho c^2\gamma\left[\left(\Omega^2\frac{R^3}{3} + (AU)^2\frac{R}{2}\right)\sum_{i=o}^{K}\theta_{is} SIN\, i\Psi\right]$$

$$+\frac{1}{2}\rho c^2\gamma\left(\Omega R^2\frac{(AU)}{2}\sum_{i=o}^{K}\theta_{ic}\left[SIN(i+1)\Psi - SIN(i-1)\Psi\right]\right)$$

$$+\frac{1}{2}\rho c^2\gamma\left(\Omega R^2\frac{(AU)}{2}\sum_{i=o}^{K}\theta_{is}\left[COS(i-1)\Psi - COS(i+1)\Psi\right]\right)$$

$$-\frac{1}{2}\rho c^2\gamma\left([AU]^2\frac{R}{4}\sum_{i=o}^{K}\theta_{ic}\left[COS(i+2)\Psi + COS(i-2)\Psi\right]\right)$$

$$-\frac{1}{2}\rho c^2\gamma\left((AU)^2\frac{R}{4}\sum_{i=o}^{K}\theta_{is}\left[SIN(i+2)\Psi+SIN(i-2)\Psi\right]\right)$$

$$-\frac{1}{2}\rho c^2\gamma\left(\Omega\frac{R^2}{2}(GU)+R^3\frac{\Omega^2}{3}\sum_{i=o}^{K}i\left(-\beta_{ic}SIN\,i\Psi+\beta_{is}COS\,i\Psi\right)\right)$$

$$-\frac{1}{2}\rho c^2\gamma(AU)(GU)R\,SIN\Psi$$

$$-\frac{1}{2}\rho c^2\gamma(AU)R^2\frac{\Omega}{2}\sum_{i=o}^{K}\frac{-i\beta_{ic}}{2}\left(\left[COS(i-1)\Psi-COS(i+1)\Psi\right]\right)$$

$$-\frac{1}{2}\rho c^2\gamma(AU)R^2\frac{\Omega}{2}\sum_{i=o}^{K}i\beta_{is}\left[SIN(i+1)\Psi-SIN(i-1)\Psi\right]$$

$$+\frac{1}{2}\rho c^2Q\left(\Omega^2\frac{R^3}{3}+(AU)^2\frac{R}{2}\right)\sum_{i=o}^{K}\frac{\theta_{ic}^2}{2}\left(COS\,2i\Psi+1\right)$$

$$+\frac{1}{2}\rho c^2Q\left(\Omega^2\frac{R^3}{3}+(AU)\frac{2R}{2}\right)\sum_{i=o}^{K}\theta_{ic}\theta_{is}SIN\,2i\Psi$$

$$+\frac{1}{2}\rho c^2Q\left(\Omega^2\frac{R^3}{3}+(AU)^2\frac{R}{2}\right)\sum_{i=o}^{K}\frac{\theta_{is}^2}{2}\left(1-COS\,2i\Psi\right)$$

$$+\frac{1}{2}\rho c^2Q\Omega R^2\frac{(AU)}{2}\sum_{i=o}^{K}\theta_{ic}^2\left(\frac{1}{2}\left[SIN(2i+1)\Psi-SIN(2i-1)\Psi\right]+SIN\Psi\right)$$

$$+\frac{1}{2}\rho c^2Q\Omega R^2\frac{(AU)}{2}\sum_{i=o}^{K}\theta_{ic}\frac{\theta_{is}}{2}\left[COS\,(2i-1)\Psi-COS(2i+1)\Psi\right]$$

$$+\frac{1}{2}\rho c^2Q\Omega R^2\frac{(AU)}{2}\sum_{i=o}^{K}\theta_{is}^2\left(SIN\Psi-\frac{1}{2}\left[SIN\,(2i+1)\Psi-SIN\,(2i-1)\Psi\right]\right)$$

$$-\frac{1}{2}\rho c^2 Q(AU)^2 \frac{R}{4} \sum_{i=o}^{K} \theta_{ic}^2 \left(\frac{1}{2} [COS(2i+2)\Psi + COS(2i-2)\Psi] + COS2\Psi \right)$$

$$-\frac{1}{2}\rho c^2 Q(AU)^2 \frac{R}{2} \sum_{i=o}^{K} \frac{\theta_{ic}\theta_{is}}{2} [SIN(2i+2)\Psi + SIN(2i-2)\Psi]$$

$$-\frac{1}{2}\rho c^2 Q(AU)^2 \frac{R}{4} \sum_{i=o}^{K} \theta_{is}^2 \left(COS2\Psi - \frac{1}{2} COS(2i+2)\Psi + COS(2i-2)\Psi \right)$$

$$-\frac{1}{2}\rho c^2 2Q \frac{\Omega R^2}{2} (GU) \sum_{i=o}^{K} \left(\theta_{ic} COS\, i\Psi + \theta_{is} SIN\, i\Psi \right)$$

$$-\frac{1}{2}\rho c^2 2Q\Omega^2 \frac{R^3}{3} \sum_{i=o}^{K} \theta_{ic} \sum_{p=o}^{W} -\frac{p\beta_{pc}}{2} [SIN(i+p)\Psi - SIN(i-p)\Psi]$$

$$-\frac{1}{2}\rho c^2 2Q\Omega^2 \frac{R^3}{3} \sum_{i=o}^{K} \theta_{ic} \sum_{p=o}^{W} \frac{p\beta_{ps}}{2} [COS(i+p)\Psi - COS(i-p)\Psi]$$

$$-\frac{1}{2}\rho c^2 2Q\Omega^2 \frac{R^3}{3} \sum_{i=o}^{K} \theta_{is} \sum_{p=o}^{W} -\frac{p\beta_{pc}}{2} [COS(i-p)\Psi - COS(i+p)\Psi]$$

$$-\frac{1}{2}\rho c^2 2Q\Omega^2 \frac{R^3}{3} \sum_{i=o}^{K} \theta_{is} \sum_{p=o}^{W} \frac{p\beta_{ps}}{2} [SIN(i+p)\Psi + SIN(i-p)\Psi]$$

$$-\frac{1}{2}\rho c^2 2Q(AU)(GU)R \sum_{i=o}^{K} \frac{\theta_{ic}}{2} [SIN(i+1)\Psi - SIN(i-1)\Psi]$$

$$-\frac{1}{2}\rho c^2 2Q(AU)(GU)R \sum_{i=o}^{K} \frac{\theta_{is}}{2} [COS(i-1)\Psi - COS(i+1)\Psi]$$

$$-\frac{1}{2}\rho c^2 \frac{2Q\,(AU)R^2}{2} \Omega \sum_{i=o}^{K} \theta_{ic} \sum_{p=o}^{W} \frac{-p\beta_{pc}}{4} [COS(i+p-1)\Psi + COS(i-p+1)\Psi]$$

$$-\frac{1}{2}\rho c^2 \frac{2Q\,(AU)R^2}{2}\,\Omega \sum_{i=o}^{K} \theta_{ic} \sum_{p=o}^{W} \frac{p\beta_{pc}}{4}\left[COS(i+p+1)\Psi + COS(i-p-1)\Psi\right]$$

$$-\frac{1}{2}\rho c^2 \frac{2Q\,(AU)R^2}{2}\,\Omega \sum_{i=o}^{K} \theta_{ic} \sum_{p=o}^{W} \frac{p\beta_{ps}}{4}\left[SIN(i+p+1)\Psi - SIN(i-p-1)\Psi\right]$$

$$-\frac{1}{2}\rho c^2 \frac{2Q\,(AU)R^2}{2}\,\Omega \sum_{i=o}^{K} \theta_{ic} \sum_{p=o}^{W} \frac{-p\beta_{ps}}{4}\left[SIN(i+p-1)\Psi - SIN(i-p+1)\Psi\right]$$

$$-\frac{1}{2}\rho c^2 \frac{2Q\,(AU)R^2}{2}\,\Omega \sum_{i=o}^{K} \theta_{is} \sum_{p=o}^{W} \frac{-p\beta_{pc}}{4}\left[SIN(i+p-1)\Psi + SIN(i-p+1)\Psi\right]$$

$$-\frac{1}{2}\rho c^2 \frac{2Q\,(AU)R^2}{2}\,\Omega \sum_{i=o}^{K} \theta_{is} \sum_{p=o}^{W} \left[SIN(i+p+1)\Psi + SIN(i-p-1)\Psi\right]$$

$$-\frac{1}{2}\rho c^2 \frac{2Q\,(AU)R^2}{2}\,\Omega \sum_{i=o}^{K} \theta_{is} \sum_{p=o}^{W} \left[COS(i-p-1)\Psi - COS(i+p+1)\Psi\right]$$

$$-\frac{1}{2}\rho c^2 \frac{2Q\,(AU)R^2}{2}\,\Omega \sum_{i=o}^{K} \theta_{is} \sum_{p=o}^{W} \frac{-p\beta_{ps}}{4}\left[COS(i-p+1)\Psi - COS(i+p-1)\Psi\right]. \quad (29)$$

In addition, there is an effect in torsion when the pitch and elastic axes are different than quarter chord, where the aerodynamic force acts. The torsional moment due to the pitch and elastic offset axes is given as

$$\frac{dM_{e_a}}{dr} = -\left(\frac{C}{4} - PA + e_a\right)\left[\frac{dL}{dr} + \frac{dD}{dr}\left(\theta - \frac{U_P}{U_T}\right)\right] \quad (30)$$

and

$$\frac{dM_{e_a}}{dr} = -\left(\frac{C}{4} - PA + e_a\right)\frac{1}{2}\,\rho c\left(a + C_D\right)\left(\theta U_T^2 - U_T U_P\right). \quad (31)$$

Performing the radial integration, again separating harmonics and letting *(C/4 − PA + e_a) = CB,*

$$M_{e_a} = - CB \frac{1}{2} \rho c \left(a + C_D\right) \left(\Omega^2 \frac{R^3}{3} + (AU)^2 \frac{R}{2}\right) \sum_{i=o}^{K} \theta_{ic} \, COS \; i\Psi$$

$$- CB \frac{1}{2} \rho c \left(a + C_D\right) \left(\Omega^2 \frac{R^3}{3} + (AU)^2 \frac{R}{2}\right) \sum_{i=o}^{K} \theta_{is} \, SIN \; i\Psi$$

$$- CB \frac{1}{2} \rho c \left(a + C_D\right) \frac{\Omega R^2}{2} (AU) \sum_{i=o}^{K} \theta_{ic} \left[SIN \; (i+1)\Psi - SIN \; (i-1) \; \Psi\right]$$

$$- CB \frac{1}{2} \rho c \left(a + C_D\right) \frac{\Omega R^2}{2} (AU) \sum_{i=o}^{K} \theta_{is} \left[COS \; (i-1)\Psi - COS \; (i+1) \; \Psi\right]$$

$$+ CB \frac{1}{2} \rho c \frac{\left(a + C_D\right)}{4} (AU)^2 R \sum_{i=o}^{K} \theta_{ic} \left[COS \; (i+2)\Psi + COS \; (i-2) \; \Psi\right]$$

$$+ CB \frac{1}{2} \rho c \frac{\left(a + C_D\right)}{4} (AU)^2 R \sum_{i=o}^{K} \theta_{is} \left[SIN \; (i+2)\Psi + SIN \; (i-2) \; \Psi\right]$$

$$+ CB \frac{1}{2} \rho c \left(a + C_D\right) \Omega^2 \frac{R^2}{2} (GU)$$

$$+ CB \frac{1}{2} \rho c \left(a + C_D\right) R^3 \frac{\Omega^2}{3} \sum_{i=o}^{K} i \left(- \beta_{ic} \, SIN \; i\Psi + \beta_{is} \, COS \; i\Psi\right)$$

$$+ CB \frac{1}{2} \rho c \left(a + C_D\right) (AU) \; (GU) \; R \; SIN \; \Psi$$

$$+ CB \frac{1}{2} \rho c \left(a + C_D\right) (AU) \; R^2 \frac{\Omega}{2} \sum_{i=o}^{K} \frac{-i\beta_{ic}}{2} \left[COS \; (i-1)\Psi - COS \; (i+1)\Psi\right]$$

$$+ CB \frac{1}{2} \rho c \left(a + C_D\right) (AU) \; R^2 \frac{\Omega}{2} \sum_{i=o}^{K} \frac{i\beta_{is}}{2} \left[SIN \; (i+1)\Psi - SIN \; (i-1)\Psi\right] . \qquad (32)$$

The rotor blade flapping equation of motion is

$$I_B \frac{d^2\beta}{dt^2} + C_B \frac{d\beta}{dt} + K_B \beta = \sum_{i=o}^{K} H_{ic} \, COS \, i\Psi + H_{is} \, SIN \, i\Psi \,, \tag{33}$$

where I_B = flap 2nd moment, C_B = flap damping, K_B = flap spring, and H_{ic} and H_{is} = flap moment forcing (cosine and sine).

Let

$$\beta = \sum_{i=o}^{K} \beta_{ic} \, COS \, i\Psi + \beta_{is} \, SIN \, i\Psi \,, \tag{34}$$

$$\frac{d\beta}{dt} = \sum_{i=o}^{K} -i\Omega\beta_{ic} \, SIN \, i\Psi + i\Omega\beta_{is} \, COS \, i\Psi \,, \tag{35}$$

Substituting in Equation 3 and equating *SIN* and *COS* terms on both sides of the equal sign,

$$-I_\beta \beta_{ic} \Omega^2 + C_\beta \beta_{is} \, i\Omega + K_\beta \beta_{ic} = H_{ic} \tag{37}$$

and

$$-I_\beta \beta_{is} \Omega^2 + C_\beta \beta_{ic} \, i\Omega + K_\beta \beta_{is} = H_{is} \,. \tag{38}$$

and

$$\frac{d^2\beta}{dt^2} = \sum_{i=o}^{K} (-i\Omega)^2 \, \beta_{ic} \, COS \, i\Psi - (-i\Omega)^2 \, \beta_{is} \, SIN \, i\Psi \,. \tag{36}$$

Let

$$H_{ic} = H_{ic-} + \beta_{is} \, LA_{ic} \tag{39}$$

and

$$H_{is} = H_{is-} + \beta_{ic} \, LA_{is} \,, \tag{40}$$

where $\beta_{is}(LA)_{ic}$ = aero coefficient of the $COS i\Psi$ terms and $\beta_{ic}(LA)_{is}$ = aero coefficient of the $SIN i\Psi$ terms.

Taking these terms over to the left-hand side in Equations 37 and 38 results in

$$- I_\beta \beta_{ic} \Omega^2 + (C_\beta i\Omega - LA_{ic}) \beta_{is} + K_\beta \beta_{ic} = H_{ic-} \tag{41}$$

and

$$- I_\beta \beta_{is} \Omega^2 + (-C_\beta i\Omega - LA_{is}) \beta_{ic} + K_\beta \beta_{is} = H_{is-} . \tag{42}$$

From Equations 41 and 42, the blade flapping responses β_{ic} and β_{is} can be determined.

Notice that the dynamic blade flap response feeds back into Equation 6. This means that the blade flap response changes the aerodynamic forcing function which in turn means that the dynamic blade flap motion will change. Therefore, there is nonlinear coupling continually going on, and the analysis should be iterated until a solution is obtained. The analysis does indeed perform this iterative process during the trim routine.

The dynamic blade equations of motion in torsion have the same form as that for flap, and elastic blade pitch occurs, having harmonic terms θ_{eic} and θ_{eis}. These elastic blade pitch motions feed back into Equation 7 and also after the aerodynamic forcing functions. In the case of torsion, it is more powerful than the flap contribution because it gets directly into the angle of attack, so that small torsional deflections can cause large changes in the blade aerodynamic forces.

4. APPLICATION OF THE ANALYSIS FOR A UH-60A HELICOPTER WITH A DAMAGED MAIN ROTOR BLADE

For the purposes of this report, the harmonic forcing functions derived in Section 3 are applied at the hub of the main rotor of a UH-60A helicopter, and the helicopter's dynamic response is calculated. Vibrations are calculated in the cockpit, assuming the fuselage to be a rigid body with six degrees of freedom (i.e., longitudinal, lateral, vertical, roll, pitch, and yaw motions of the helicopter about its center of gravity).

The sources of the rotor blade and fuselage characteristics data come from a combination of special dynamics data requested from the manufacturer and from general technical manual data from the manufacturer. There is no one place from which an analyst can obtain the data, but it is a matter of digging and searching into all kinds of documents or phoning the manufacturer for information.

The damage that is assumed is the removal of sections of the blade tip ranging from 0% to 48% of the blade. The loss of blade sections results in shortening, reduction of weight, reduction of the blade's first and second moments, and the increase of the blade's first flap frequency. Table 1 shows the changes of blade properties as a function of blade loss. The damage is applied to one of the four-bladed rotor sets with the helicopter flying at 160 knots.

The cockpit vibrations that result from the blade damage defined from Table 1 are shown in Figure 2. These vibrations are resultant vibrations, the vector sum of vertical, longitudinal, and lateral vibrations.

It is seen in Figure 2 that the cockpit vibrations vary up to 2 Gs at a frequency equal to the rotor RPM, called 1/REV, in the cockpit when 48% of one blade is lost. Reduced amounts of 2/REV, 3/REV, 4/REV, and 5/REV vibrations are present. 1/REV means a vibration equal to the rotor speed, 2/REV means a vibration at two times the rotor speed, and so on up the line to the higher /REV values.

5. DISCUSSION OF RESULTS

These results show the significance of an unbalanced rotor on vibrations in the cockpit of a helicopter. When a rotor is balanced, inherent vibrations are transmitted into the fixed system fuselage at frequencies that are integer multiples of the number of blades in the rotor. This means for the case of the Black Hawk helicopter with four blades, only 4/REV, 8/REV, and 12/REV vibrations can be transmitted into the fuselage for an undamaged rotor. Transmission of all other frequencies is zero.

For the Black Hawk, the 4/REV frequency with no damage is .072 Gs, which is insignificant on the scale of vibrations shown in Figure 2. The 8/REV frequency vibrations are even less.

For blade damage, however, loss of blade sections causes a steady unbalanced load in the rotating system, which transfers into the fixed fuselage system as a 1/REV. When 48% of the outboard section of one blade is removed, the vibrations are 2 Gs, a very severe condition for human tolerance. The

Table 1. Rotor Blade Physical Properties

Tip Loss (%)	Blade Radius (ft)	Weight (lb)	1st Moment (lb-sec^2)	2nd Moment (lb-ft-sec^2)
0	26.83	211.00	87.90	1,572
2	26.29	206.78	84.42	1,479
4	25.75	202.56	81.01	1,391
6	25.22	198.34	77.67	1,305
8	24.68	194.12	74.40	1,224
10	24.14	189.90	71.20	1,146
12	23.61	185.68	68.07	1,071
14	23.07	181.46	65.01	1,000
16	22.53	177.24	62.02	931
18	22.00	173.02	59.10	866
20	21.46	168.80	56.25	805
22	20.92	164.58	53.48	746
24	20.39	160.36	50.77	690
26	19.85	156.14	48.13	637
28	19.31	151.92	45.57	586
30	18.78	147.70	43.07	539
32	18.24	143.48	40.64	494
34	17.70	139.26	38.29	452
36	17.17	135.04	36.00	412
38	16.63	130.82	33.79	374
40	16.09	126.60	31.64	339
42	15.56	122.38	29.57	306
44	15.02	118.16	27.56	276
46	14.48	113.94	25.63	247
48	13.95	109.72	23.76	221

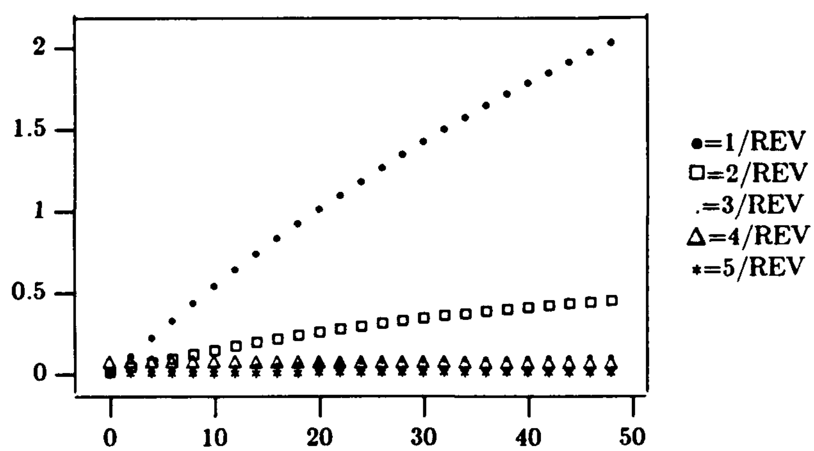

Figure 2. Cockpit vibrations (Gs) vs. percentage of blade lost.

higher harmonics areless severe in magnitude but may be just as effective in debilitating a human if human organs are resonant to these higher frequencies (Linder 1959).

With blade damage, the 1/REV, 2/REV, and 3/REV vibrations are all higher than the ambient 4/REV vibrations (no damage).

The computer program is an ongoing in-house development program conducted by the author. Several papers have been presented by the author wherein results were generated using this computer program (Fries 1990a, 1990b, 1990c).

The computer program runs by establishing a steady-state trim condition and the damage is imposed on the main rotor. The vibrations that arise are instantaneous in nature, of just one rotor revolution duration after the damage occurs. The program does not analyze the helicopter vibrations after the damage for long periods of time. To do this, we know that the damage will cause the helicopter to go out of trim and the pilot would have to compensate with the controls in some manner.

The program is of first order accuracy and is considered to be a first order approximation to the vibrations that exist for a helicopter with a damaged rotor. The aerodynamics are of first order, the second order terms are neglected, and the airframe is a rigid body not considering flexibility or natural modes. The program is the first attempt at understanding this vibration problem and ongoing work is needed to enhance the program. The advantage of the program is that it is relatively small and easy to use to get quick results as opposed to very large analyses existing at universities and helicopter manufacturers that require years of experience and many months to exercise a specific helicopter model.

The program has approximately 700 lines of code in BASIC language that runs on the author's Northgate Elegance - 425i personal computer. It is available from the author to anyone who wishes to use it.

6. CONCLUSIONS

A workable vibration analysis that can quantify aircraft vibrations for a variety of main rotor damages is available. For this report, only one type of damage was considered, that of the loss of various amounts of the outboard sections of one blade.

This analysis brings up the question of human tolerance to vibrations and the effect on a pilot's ability to fly the aircraft from a physiological point of view.

Another question is the control authority remaining to the pilot with blade loss, and then there is the further question of the aircraft's stability characteristics after damage.

This computer program is a useful tool for vulnerability analysis and may be used to investigate the many factors that could lead to helicopter attrition caused by combat damage.

7. REFERENCES

Barnes, M. Aerodynamics of V/STOL Flight. New York: Academic Press, Inc., 1967.

Chopra, I. Notes on Helicopter Dynamics. College Park, MD: University of Maryland, 1992.

Fries, J. "Helicopter Rotor Blade Ballistic Damage Effects on Helicopter Dynamic Characteristics," Presentation to 18th Meeting of WTP-6, China Lake, CA, April 1990a.

Fries, J. "The Effect of Structural Variations on the Dynamic Characteristics of Helicopter Rotor Blades," Presented at the 31st AIAA SDM Conference, Long Beach, CA, April 1990b.

Fries, J. "Helicopter Rotor Blade Ballistic Damage Effects on Helicopter Dynamic Characteristics," Presented to Army Science Conference, Durham, NC, June 1990c.

Linder, G. S. "Effects of Mechanical Vibration on Humans: North America Aviation Report ADA950209, Los Angeles, CA, 1959.

INTENTIONALLY LEFT BLANK.

APPENDIX:

DESCRIPTION OF THE COMPUTER PROGRAM TO PREDICT HELICOPTER VIBRATIONS FOR UNDAMAGED AND DAMAGED MAIN ROTOR BLADES

INTENTIONALLY LEFT BLANK.

A-1. DESCRIPTION OF THE RTVIB20 COMPUTER PROGRAM

The computer code first performs a trim analysis for forward speed level flight by computing the aerodynamic forces in the manner described in Section 3. From these forces, a balance is struck in the vertical and horizontal directions so that level flight is maintained at a constant forward speed. This balance is maintained by adjusting the blade collective pitch and the aircraft pitch attitude by iteration until a balanced condition is obtained.

The physical properties input into the program are listed in Section A-2 of this appendix, along with the computer code line numbers. The numerical values listed are for the UH-60A helicopter and come from such a wide variety of sources that they are not listed. They come by word of mouth through telephone conversations with the manufacturer, or by special correspondence, or by digging out data from the manufacturer's technical manuals. Once a trimmed condition is achieved, the program goes on to calculate fixed system vibrations at a position on the fuselage as specified by the user. In this report, the cockpit location was chosen.

Two iterative trim loops start at lines 521 and 530 of the code and finish at lines 1320 and 2350. Within the inner loop, the blade collective pitch is varied, and in the outer loop the aircraft's pitching attitude is changed until a vertical and horizontal force balance is achieved.

When the helicopter is flying straight and level, the program will perform either an undamaged or damaged main rotor vibration analysis. Whichever path is taken depends on the physical input data on lines 3060 to 3090. On these input lines there are inputs R, IB, SB, W, A, CD, EB, WN, ITH, CM, A1, and Q variables on N separate lines to represent individual blades. That is, on line 3060 we have this data for blade 1, line 3060 for blade 2, and so on for a four-bladed rotor. The last line is line 3090. For an undamaged blade, the input values on these lines will be identical to the corresponding values input to lines 50, 300, 360, 440, or 500, as described in Section A-2.

For an undamaged blade, all the input parameters for one variable on each of these lines (3060–3090 for a four-bladed rotor) are identical. When one of the blades is damaged in some way, the physical properties will change and this will be reflected in a change in one or more of the input parameters on one of these particular lines. For instance, a hole through one blade will require IB, SB, W, A, CD, WN, ITH, CM, A1, and Q on one particular line for the blade to be changed to account for damage (see input variable definitions).

The fixed system cockpit vibrations produced by blade shears and moments for undamaged and damaged blades are calculated using the computer code and are reported in Section A-4 for the example of the UH-60A helicopter.

A-2. INPUT VARIABLES OF THE COMPUTER CODES

Variable Inputs	Variable Input Name	Unit of Measurement	Line No.	Numerical Input
AT	Pressure altitude	ft	50	4,000
T	Outside temperature	deg F	50	95
CH	Blade chord = C	inches	300	20.88
R	Blade tip radius	ft	300	26.83
TT	Blade geometric twist	deg/ft	300	.671
OM	Rotor speed	rpm	300	258.
V	Aircraft forward speed	knots	300	160.
VC	Vertical climb rate	knots	300	0.
GA	Rotor shaft tilt = G, + into wind	deg	300	3
PI	Aircraft pitch, + into wind. Note: not 3.14	deg	300	10.49
CD	Blade drag coefficient, steady	nd	300	.04
GW	Aircraft gross weight	lb	360	16,260.
TO	Blade collective pitch	deg	360	37.29
T1	Blade lateral cyclic pitch	deg	360	.88
T2	Blade longitudinal cyclic pitch	deg	360	-10.79
N	Number of blades per rotor	nd	360	4
FE	Aircraft profile flat plate area	ft^2	360	74.55
IB	Blade 2nd flap moment	$lb\text{-}sec^2\text{-}ft$	440	1,570
SB	Blade lst flap moment	$lb\text{-}sec^2$	440	87.90
W	Blade weight	lb	440	211
EB	Blade flap offset from center of rotation	in	440	21.98
PA	Blade pitch axis from leading edge	in	500	5.22

Variable Inputs	Variable Input Name	Unit of Measurement	Line No.	Numerical Input
WN	Blade lst torsion natural frequency normalized by rotor speed	nd	500	3.728
ITH	Blade pitch inertia	lb-sec^2-ft	500	.865
CM	Blade aerodynamic pitch coefficient steady	nd	500	-.04
MC	Blade chordwise mass center from l.e.	in	500	0
A1	Blade linear aerodynamic pitch coefficient, multiplies angle of attack	nd	500	−.08
EA	Blade elastic axis from l.e.	in	500	5.22
Q	Blade non-linear aerodynamic pitch coefficient, multiplies angle of attack squared	nd	500	0
IY	Aircraft pitch inertia	lb-sec^2-ft	5680	60,731
IX	Aircraft roll inertia	lb-sec^2-ft	5680	4,118
XX	Longitudinal distance from rotor hub to the place where vibrations are calculated	in	5680	134
YY	Lateral distance to vibration location	in	5680	20
ZZ	Vertical distance to vibration location as above	in	5680	−100
EX	Longitudinal distance from the rotor hub to the aircraft c.g.	in	5680	11
EZ	Vertical distance from rotor hub to the aircraft c.g.	in	5680	63

A-3. DESCRIPTION OF COMPUTER PROGRAM OUTPUT

Only pertinent outputs will be given. There is much output which is intermediate in nature so excerpts will be presented.

After the program iterates on a trim condition, a final set of values of blade collective pitch, aircraft pitch attitude, vertical force, and downwash velocity are produced. The results are given in

Section A-4 for the undamage case for the UH-60A flying at 160 knots. Also presented in Section A-4 are the results of calculations of the vertical fixed system hub shears and the in-plane hub shears. The example case is for an undamaged rotor condition, in which only the four/rev shears are significant for a four-bladed rotor. For a damaged case rotor blade, all the harmonics may be significant. The 1/REV in-plane shears only are given, and we see that for the undamaged case these shears are small; however, for a damaged case, the steady damage in the rotating system translates into 1/REV fixed system shears that are significant.

Fixed system 4/REV hub moments are given in Section A-4. Again, only the 4/REV values are listed because only these are transmitted into the fixed system for an undamaged rotor. Also, in Section A-4 are listed the quasi-theoretical moments based upon the expected output at specific azimuth positions. These are used as a check against the values that are calculated in the stepwise incrementing around the azimuth. These theoretical moments come from the harmonic closed form hand calculations from which the magnitudes at specific azimuth positions are known. For instance, at 1/REV, we know the cosine amplitude at zero azimuth is either maximum or minimum and the sine amplitudes are either maximum or minimum at the azimuth position of 90 degrees.

The final output consists of cockpit vibrations which are also listed in Section A-4. These are the base case vibrations for an undamaged rotor against which damage cases can be compared. They are broken down into cosine and sine components of vibration in the longitudinal, lateral, and vertical directions. Again, here only the 4/REV vibrations are transmitted from the blade rotating system into the fuselage fixed system because of a balanced rotor when no damage is present.

Note that some of the variable output names in Section A-4 are identical in physical meaning, but only in a programming sense. That is, they are variables in the code that are printed out sequentially in time and are reused at a later point in the execution of the program. The line number on which the variable rests determines the physical quantity that is printed.

A-4. OUTPUT VARIABLES OF THE COMPUTER CODE

Variable Output	Variable Output Name	Unit of Measurement	Line No.	Numerical Outputs
TO	Blade collective pitch	deg	1171 1241	38.57 38.57
PI	Aircraft pitch into wind	deg	1171 1241	8.32 8.32
FV*	Vertical force	lb	1271	15,948.81
GW	Gross weight	lb	1271	16,260.
U	Downwash velocity	ft/sec	1271	49.71
	Fixed System Vertical Forces			
I (4/REV)	Harmonic number	nd	4680	1 to 6
ACX	Max. cosine amplitude	lb	4680	212.70
ZCX	Azimuthal position of ACX	deg	4680	45
ACN	Min. cosine amplitude	lb	4680	−212.70
ZCN	Azimuthal position of ACN	deg	4680	0
ASX	Max. sine amplitude	lb	4690	5.87
ZSX	Azimuthal position of ASX	deg	4690	22.5
ASN	Min. sine amplitude	lb	4690	−5.87
ZSN	Azimuthal position of ASN	deg	4690	67.5
	In-Plane Fixed System Forces, 1/REV			
FXC	Last longitudinal cosine force calculated about the azimuthal steps	lb	4990	.5019
ACX	Max. longitudinal cosine force	lb	4990	.753
XCX	Azimuthal position of deg ACX	deg	4990	49.09
ACN	Min. longitudinal cosine force	lb	4990	−.753
XCN	Azimuthal position of ACN	deg	4990	212.7

*FV = N*TH*COS(GA+PI)

Variable Output	Variable Output Name	Unit of Measurement	Line No.	Numerical Outputs
FYS	Last lateral sine force calculated about the azimuthal steps	lb	5000	−.585
ASX	Max. lateral sine force	lb	5000	.753
XSX	Azimuthal position of ASX	deg	5000	130.9
ASN	Min. lateral sine force	lb	5000	−.765
XSN	Azimuthal position of ASN	deg	5000	310.9
		Fixed System Moments		
I (4/REV)	Harmonic number	nd	5520	1 to 6
XSX	Max. sine rolling moment	ft-lb	5520	1,014.56
PSX	Azimuth position of XSX	deg	5520	67.5
XSN	Min. sine rolling moment	ft-lb	5520	−1,014.56
PSN	Azimuth position of XSN	deg	5520	22.5
MXS	Last calculated sine moment about the azimuth	ft-lb	5520	−.0081
XCX	Max. cosine rolling moment	ft-lb	5530	2,485.99
PCX	Azimuth position of XCX	deg	5530	0
XCN	Min. cosine rolling moment	ft-lb	5530	−2,485.99
PCN	Azimuth position of XCN	deg	5530	45
MXC	Last calculated cosine moment about the azimuth	ft-lb	5530	2,485.99
YSX	Max. sine pitching moment	ft-lb	5540	2,611.93
QSX	Azimuth position of YSX	deg	5540	22.5
YSN	Min. sine pitching moment	ft-lb	5540	−2,611.93

Variable Output	Variable Output Name	Unit of Measurement	Line No.	Numerical Outputs
QSN	Azimuth position of YSN	deg	5540	67.5
MYS	Last calculated sine pitching moment about the azimuth	ft-lb	5540	.208
YCX	Max. cosine pitching moment	ft-lb	5550	1,083.36
QCX	Azimuth position of YCX	deg	5550	0
YCN	Min. cosine pitching moment	ft-lb	5550	−1,083.36
QCN	Azimuth position of YCN	deg	5550	45
MYC	Last calculated cosine pitching moment about azimuth	ft-lb	5550	1,083.36

Theoretical Fixed System Moment Values

I (4/REV)	Harmonic number	nd	5630	1 to 9
XMS	Sine rolling moment	ft-lb	5630	−1,014.56
YMS	Sine pitching moment	ft-lb	5630	2,611.93
XMC	Cosine rolling moment	ft-lb	5630	2,485.99
YMC	Cosine pitching moment	ft-lb	5630	1,083.36

Cockpit Vibrations

I (4/REV)	Harmonic number	nd	5800	1 to 10
X2C	Longitudinal cosine	Gs	5800	.00140
X2S	Longitudinal sine	Gs	5800	.00412
Y2C	Lateral cosine	Gs	5800	.0578
Y2S	Lateral sine	Gs	5800	−.0235
Z2C	Vertical cosine	Gs	5800	.0367
Z2S	Vertical sine	Gs	5800	.00342

INTENTIONALLY LEFT BLANK.

No. of Copies	Organization
2	Administrator Defense Technical Info Center ATTN: DTIC-DDA Cameron Station Alexandria, VA 22304-6145
1	Commander U.S. Army Materiel Command ATTN: AMCAM 5001 Eisenhower Ave. Alexandria, VA 22333-0001
1	Director U.S. Army Research Laboratory ATTN: AMSRL-D 2800 Powder Mill Rd. Adelphi, MD 20783-1145
1	Director U.S. Army Research Laboratory ATTN: AMSRL-OP-CI-AD, Tech Publishing 2800 Powder Mill Rd. Adelphi, MD 20783-1145
2	Commander U.S. Army Armament Research, Development, and Engineering Center ATTN: SMCAR-IMI-I Picatinny Arsenal, NJ 07806-5000
2	Commander U.S. Army Armament Research, Development, and Engineering Center ATTN: SMCAR-TDC Picatinny Arsenal, NJ 07806-5000
1	Director Benet Weapons Laboratory U.S. Army Armament Research, Development, and Engineering Center ATTN: SMCAR-CCB-TL Watervliet, NY 12189-4050
(Unclass. only) 1	Commander U.S. Army Rock Island Arsenal ATTN: SMCRI-IMC-RT/Technical Library Rock Island, IL 61299-5000
1	Director U.S. Army Aviation Research and Technology Activity ATTN: SAVRT-R (Library) M/S 219-3 Ames Research Center Moffett Field, CA 94035-1000

No. of Copies	Organization
1	Commander U.S. Army Missile Command ATTN: AMSMI-RD-CS-R (DOC) Redstone Arsenal, AL 35898-5010
1	Commander U.S. Army Tank-Automotive Command ATTN: ASQNC-TAC-DIT (Technical Information Center) Warren, MI 48397-5000
1	Director U.S. Army TRADOC Analysis Command ATTN: ATRC-WSR White Sands Missile Range, NM 88002-5502
1	Commandant U.S. Army Field Artillery School ATTN: ATSF-CSI Ft. Sill, OK 73503-5000
(Class. only) 1	Commandant U.S. Army Infantry School ATTN: ATSH-CD (Security Mgr.) Fort Benning, GA 31905-5660
(Unclass. only) 1	Commandant U.S. Army Infantry School ATTN: ATSH-CD-CSO-OR Fort Benning, GA 31905-5660
1	WL/MNOI Eglin AFB, FL 32542-5000
	Aberdeen Proving Ground
2	Dir, USAMSAA ATTN: AMXSY-D AMXSY-MP, H. Cohen
1	Cdr, USATECOM ATTN: AMSTE-TC
1	Dir, ERDEC ATTN: SCBRD-RT
1	Cdr, CBDA ATTN: AMSCB-CI
1	Dir, USARL ATTN: AMSRL-SL-I
10	Dir, USARL ATTN: AMSRL-OP-CI-B (Tech Lib)

No. of Copies	Organization
3	Commander USA Aviation Systems Command ATTN: AMSAV-ESC, G. Kovacs SAFE-AV-BH-T, R. Olson SAFE-AV-AAH-SA, D. Roby 4300 Goodfellow Blvd. St. Louis, MO 63120-1798
2	Commander AATD ATTN: AMSAT-R-TF, G. Hufstetler SAVRT-TY-ASV, H. Reddick USAATCOM Ft. Eustis, VA 23604-5577
1	Commander ASC ATTN: ASC/XRM, G. Bennett AFSC Headquarters Wright-Patterson AFB, OH 45433-6503
1	Commander WRDC ATTN: WL/FIVST, M. Lentz AFSC Headquarters Wright-Patterson AFB, OH 45433-6553
1	Commander ATTN: ASC/XRYA, K. McArdle Eglin AFB, FL 32542
2	Commander Naval Surface Warfare Center ATTN: Code G-13, T. Wasmund D. Dickinson Dahlgren, VA 22448
1	McDonnell Douglas Helicopter Company ATTN: William Sims 5000 E. McDowell Rd. Mesa, AZ 85205
1	Boeing Helicopters Division ATTN: N. Caravasos P.O. Box 16858 Philadelphia, PA 19142

No. of Copies	Organization
1	Silkorsky Aircraft Mail Stop, Z101A ATTN: G. Burblis 6900 Main Street Stratford, CT 06601-1381
	Aberdeen Proving Ground
1	Dir, USAMSAA ATTN: AMXSY-AD, C. Alston

USER EVALUATION SHEET/CHANGE OF ADDRESS

This Laboratory undertakes a continuing effort to improve the quality of the reports it publishes. Your comments/answers to the items/questions below will aid us in our efforts.

1. ARL Report Number ARL-TR-75 Date of Report February 1993

2. Date Report Received ______________________

3. Does this report satisfy a need? (Comment on purpose, related project, or other area of interest for which the report will be used.) ______________________

4. Specifically, how is the report being used? (Information source, design data, procedure, source of ideas, etc.) ______________________

5. Has the information in this report led to any quantitative savings as far as man-hours or dollars saved, operating costs avoided, or efficiencies achieved, etc? If so, please elaborate. ______________________

6. General Comments. What do you think should be changed to improve future reports? (Indicate changes to organization, technical content, format, etc.) ______________________

CURRENT ADDRESS

Organization

Name

Street or P.O. Box No.

City, State, Zip Code

7. If indicating a Change of Address or Address Correction, please provide the Current or Correct address above and the Old or Incorrect address below.

OLD ADDRESS

Organization

Name

Street or P.O. Box No.

City, State, Zip Code

(Remove this sheet, fold as indicated, staple or tape closed, and mail.)

DEPARTMENT OF THE ARMY

OFFICIAL BUSINESS

BUSINESS REPLY MAIL
FIRST CLASS PERMIT No 0001, APG, MD

Postage will be paid by addressee

NO POSTAGE
NECESSARY
IF MAILED
IN THE
UNITED STATES

Director
U.S. Army Research Laboratory
ATTN: AMSRL-OP-CI-B (Tech Lib)
Aberdeen Proving Ground, MD 21005-5066